

Detection of Nitrous Oxide (N₂O) at sub-ppmv using Intracavity Absorption Spectroscopy (ICAS)

Jonas K. Valiunas, George Stewart and Gautam Das

Abstract— The authors demonstrate a fibre laser system for detection of the greenhouse gas, nitrous oxide (N₂O), at sub-ppmv concentration levels. The fibre laser is stabilized by a saturable absorber. The sensitivity is enhanced by multiple circulations of ASE light under threshold conditions, and multi-longitudinal mode oscillation of the laser. An intra-cavity Herriott cell of effective path length 30 m was used to detect the P (12) rotational line of N₂O at ~1522.20 nm.

Index Terms—Laser spectroscopy, intracavity spectroscopy, fibre laser, fibre sensors, gas sensor

Nitrous oxide (N₂O) gas is a minor constituent in the Earth's atmosphere (~300 ppbv), but the levels of N₂O are rising due to human augmentation of the nitrogen cycle. N₂O contributes to the destruction of the stratospheric ozone layer, increases the greenhouse effect in the atmosphere, and has a direct impact on human health. As a greenhouse gas (GHG), it is ~ 300 times more destructive than carbon dioxide (CO₂). Agricultural fertilizers are major sources of N₂O [1;2]. As the global population continues to increase, the use of fertilizer will also increase to meet the demand for food.

The current technology used to quantify the emission of N₂O from agricultural fields caused by fertilizer application is complex and expensive. In most cases, it involves collecting emitted gases and analyzing them using Gas Chromatography or Fourier Transform Infrared Spectroscopy in the laboratory, or using expensive laser spectroscopy methods including cavity ring down spectroscopy and, more commonly, cryo-cooled Pb-salt tunable diode laser spectroscopy [2]. A highly sensitive technique to provide real-time analysis at ambient temperature is in demand. Further, N₂O has weak absorption lines in the 1.55 μm wavelength band, which falls within the emission band of Erbium-doped fibre (EDF). A real-time analyzer in this band will not only be able to operate at room temperature but can also be developed with the available optical and electronic components used in the

telecommunication industry. The resulting system will be compact and cost effective, and it will be possible for the system to incorporate a multipoint sensor using fibre optic networking [3].

A number of articles about N₂O have identified the overtones of the characteristic absorption (fundamental) and the combinations of the overtones in the near infrared (NIR) region (1-2 μm) of the electromagnetic spectrum using Fourier transform absorption spectroscopy [4-9], cavity ring down spectroscopy [10-12] and intracavity laser absorption spectroscopy [13]. N₂O gas has three fundamental infrared active absorption bands: $\nu_1= 1285 \text{ cm}^{-1} \sim 7.8 \mu\text{m}$; $\nu_2= 589 \text{ cm}^{-1} \sim 17 \mu\text{m}$; and $\nu_3= 2224 \text{ cm}^{-1} \sim 4.5 \mu\text{m}$. The gas has overtones of the fundamental absorption bands and rovibrational transitions in the near-infrared region (1-2 μm). In this article, the authors present a technique based on intracavity absorption spectroscopy (ICAS), which can detect the weak absorption lines in the 1.52 μm P-branch of the $3\nu_3$ band for N₂O available from HITRAN [14], more specifically the P (12) rotational line at ~1522.20 nm. The technique uses the amplified spontaneous emission (ASE) present inside the laser cavity. The system was able to detect N₂O gas at sub-ppmv concentration levels.

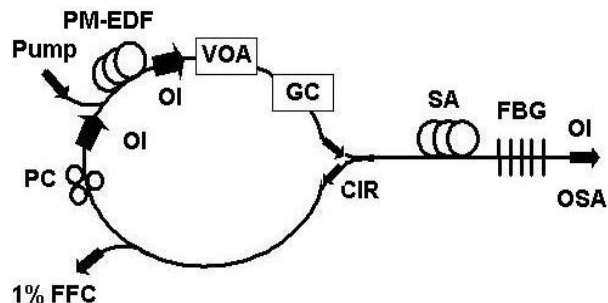


Fig.1. Schematic of the ICAS system. PUMP: 980 nm pump laser; PM-EDF: Polarization-maintaining erbium-doped fibre; VOA: Variable optical attenuator; GC: Gas cell; SA: Saturable absorber; FBG: Fibre Bragg grating; OSA: Optical spectrum analyzer; CIR: Polarization independent optical circulator; FFC: 2x2 Fused fibre coupler; PC: All-fibre polarization controller and OI: Polarization independent optical isolator.

Manuscript submitted June 26, 2015. This work was supported by the Natural Sciences and Engineering Research Council of Canada and Agrium Inc. (Corresponding author: Gautam Das)

Jonas K. Valiunas (e-mail: jvaliuna@lakeheadu.ca) and Gautam Das (e-mail: gdas@lakeheadu.ca) are with the Department of Physics, Lakehead University, 955 Oliver Road, Thunder Bay, Ontario, P7B 5E1, Canada.

George Stewart (e-mail: g.stewart@strath.ac.uk) is with the University of Strathclyde, 204 George Street, G1 1XW, Glasgow, UK.

CorActive, Canada) with length, core dimension, absorption and NA of 5 m, $3.8 \times 14.8 \mu\text{m}$, 7.2 dB/m at 980 nm and 0.15, respectively as a gain medium; a variable optical attenuator (VOA, FVA 600, EXFO) to adjust the total loss in the cavity in order to obtain the desired emission spectrum of PM-EDF; a multipass gas cell (Herriott cell) with effective path length of 30 m and volume ~ 0.9 liter; an unpumped PM-EDF of length 0.50 m as the saturable absorber (SA); a fibre Bragg grating (FBG) of reflectivity 85.16%, peak wavelength ~ 1522.22 nm and bandwidth of 0.168 nm, which was selected to match closely with the absorption peak of the N_2O gas under investigation and does not interfere with the absorption spectrum of CO_2 and H_2O ; a 1% 2×2 fused fibre coupler (FFC) to monitor the power from the resonator using a power meter; and an all-fibre polarization controller to control the polarization state of the light inside the cavity. The PM-EDF was pumped by a laser diode at 980 nm through a 980/1550-nm wavelength division multiplexer. Two polarization-independent optical isolators and a polarization-independent optical circulator guaranteed the unidirectional propagation of light inside the cavity, and an optical spectrum analyzer (OSA, ANDO) was used to collect the output of the system. The attenuator was connected by an angled connector.

The presence of the two isolators increases the stability of the cavity. Attaching the optical isolator between the pump and the attenuator reduces any back-reflection from the attenuator port. The isolator between the polarization controller and the pump eliminates the backward-propagating ASE from the PM-EDF, preventing it from reaching the FFC and the circulator.

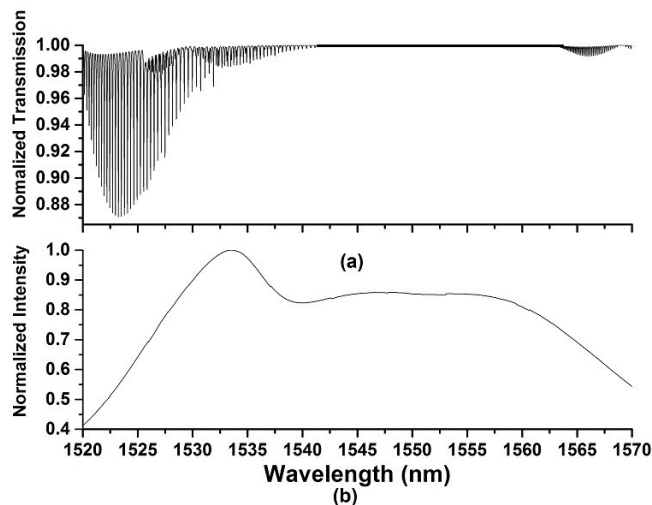


Fig. 2: (a) Theoretical absorption lines for 2% N_2O and a path length of 30 m obtained using GATS Spectral Calculator (HITRAN 2012); (b) ASE spectrum for PM-EDF for 50 mA pump current.

The total length of the laser cavity was approximately 50 m, which corresponds to a longitudinal mode spacing of ~ 4 MHz. Thus the output of the laser (at wavelength ~ 1522.22 nm) contained many closely spaced longitudinal modes. In general, a laser that contains multiple longitudinal modes is susceptible to mode-hopping from environmental fluctuations such as temperature. The transient grating formed inside the SA, due to the counter-propagating light waves, acts as a

tracking filter and stabilizes the laser by eliminating the mode-hopping. The reflection bandwidth of the transient grating is inversely proportional to the length of the SA [$\sim c/(2nL_{\text{PM-EDF}})$]; thus, by increasing the length of the SA we can obtain a very narrow-band transient grating. The drawback is that the threshold pump power of the laser increases. The use of a PM-EDF increases the stability of the transient grating. The transient grating and the FBG form a Fabry-Perot cavity, which is a resonant cavity that overlaps with the unidirectional ring cavity and serves to further stabilize the laser output. Previous authors [15;16] have reported that a multimode laser with homogeneously broadened gain bandwidth provides very high sensitivity in ICAS if the absorption linewidth is smaller than the laser linewidth.

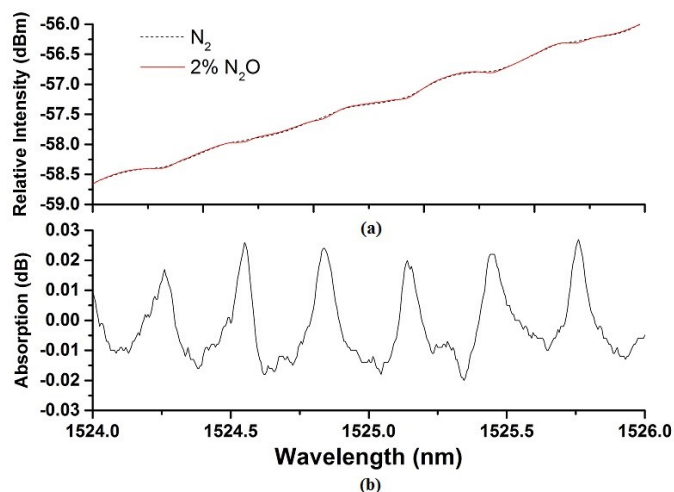


Fig. 3: (a) Transmission spectrum with the reference gas N_2 and 2% N_2O ; (b) Absorption spectrum of N_2O after subtraction from reference N_2 gas.

Before testing the fibre laser system of Figure 1, experiments were conducted on a simple fibre laser loop cavity as described in reference [17], which makes use of the ASE near threshold conditions to observe gas absorption lines with an intra-cavity cell. Here the 30 m gas cell was used along with the VOA to flatten the ASE spectrum. Figure 2 shows the theoretical absorption lines for 2% N_2O and the ASE spectrum of the fibre cavity. It is evident from Figure 2(a) that N_2O possesses relatively strong absorption lines at ~ 1522 nm, but these do not match well with the flat regions of the natural ASE spectrum of EDF as shown in Figure 2(b). The minimum concentration of the N_2O gas that this simple system (without the FBG and SA as shown in Figure 1) could detect was 2%. Figure 3(a) shows the transmission spectrum obtained from the OSA with reference gas N_2 and N_2O . Figure 3 (b) is the absorption spectrum after subtracting N_2O gas spectrum from the reference N_2 gas. Detection of lower concentrations of gases such as C_2H_2 and CO_2 were attained in [17] because of the better match between the absorption lines and the flat regions of the ASE spectrum. As indicated in Figure 2(b) the intensity of the ASE spectrum in the 1522 nm band for N_2O is much lower than that in the C and L band region and is not flat, which is one of the essential requirements for successful implementation of the method described in [17].

The experimental setup described in Figure 1 eliminated the problems described above and allowed us to detect N_2O at very low concentrations (\sim ppbv). Figure 4(a) and 4(b) show the transmission spectra of the system with the reference gas N_2 (Praxair, Canada, Research Grade, Nitrogen 6.0) and N_2O (Praxair, Canada, certified concentration of N_2O : 9.95 ppm + N_2 balance) gas for two different pump currents (I_p). The gas cell was flushed with N_2 before and after the scanning with the 10 ppm N_2O gas inside the gas cell. The transmission spectra are given as N_2^{Before} and N_2^{After} , respectively. One can obtain the absorption spectrum by subtracting the N_2O spectrum from the average of the N_2 spectra. As evident from the figures, the high enhancement was obtained when the laser was operating close to threshold condition ($I_p=130$ mA).

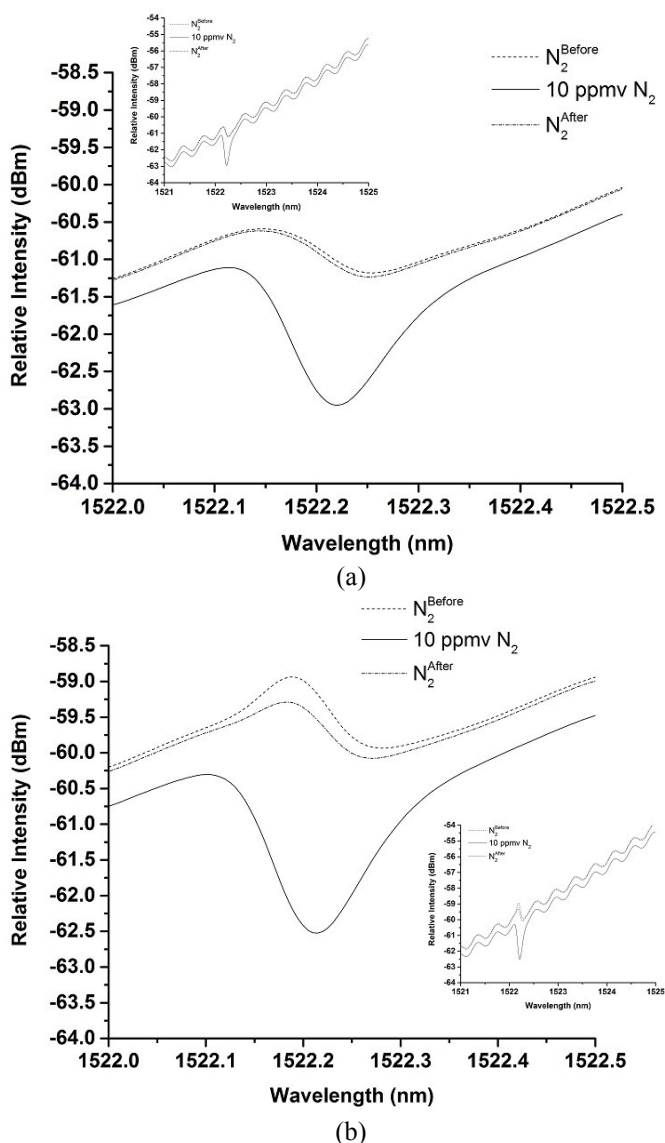


Fig. 4: Transmission spectra of the laser with reference gas N_2 and N_2O (PRAXAIR, Canada, 9.95 ppmv + N_2 balance) gas for (a) $I_p=99$ mA and (b) $I_p=130$ mA. Insets of figures are the full spectra.

In this technique the laser wavelength, which was selected by the FBG, was kept at the threshold position, so that the ASE spectrum close to the laser wavelength was almost flat

(in other words, also close to the threshold). The ASE light near the laser wavelength circulates multiple times in the cavity and enhances the effective path length. Figure 5 shows the laser output on the OSA compared with the theoretical N_2O absorption lines around 1522 nm. The laser line supports more than a thousand longitudinal modes, which is illustrated by a few vertical lines drawn inside the lasing line. A number of longitudinal-modes will disappear once they coincide with the absorption line. As the erbium-doped fiber is a homogeneous gain medium at room temperature, any small loss in the cavity will change the cavity resonance condition. Further, Baev et al. demonstrated that a multimode laser with homogeneously broadened gain medium offers a very high sensitivity due to absorption by longitudinal-modes [15]. Thus the sensitivity of detection was enhanced due to (i) multiple circulations of the ASE light inside the cavity as the laser operates close to threshold, and (ii) multi-longitudinal mode oscillation of the laser, which allows a number of cavity modes to coincide with the gas absorption lines [18]. The interference pattern visible in the transmission spectrum is due to the etalon effect between the connector and quartz windows in the gas cell. The pattern disappears in the absorption spectrum as we subtract the N_2O spectrum from the N_2 gas spectrum as reference. Further, we can operate the laser in different regimes (above, below or under threshold conditions) either by adjusting the pump current of the laser at constant attenuation or adjusting attenuation at constant pump current.

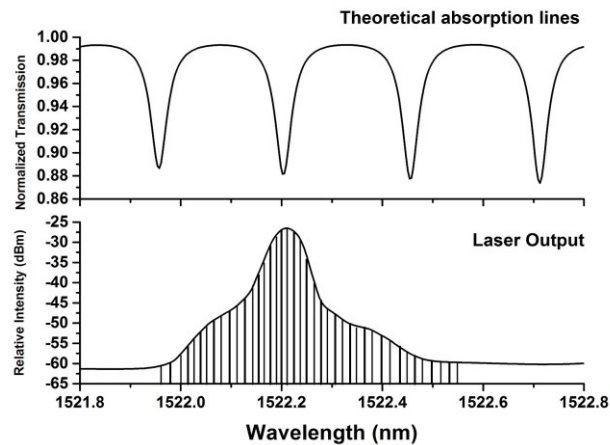


Fig. 5: Output of the laser obtained using the OSA (a few vertical lines are drawn to show multi-longitudinal mode oscillation. The separation between them is not the actual longitudinal-mode spacing) and theoretical absorption lines obtained using GATS Spectral Calculator (HITRAN 2012).

In order to study the sensitivity of the system, we prepared N_2O gas at lower concentrations from certified standard mixtures (PRAXIAR, Canada). A mass flow controller (OMEGA, model: FMA 5412) controlled by LABVIEW was used to prepare a 6 L gas mixture with N_2O and N_2 (PRAXIAR, Canada, Research grade, Nitrogen 6.0) in a 10 L Tedlar sampling bag (Cole-Parmer Canada). For example, to achieve a concentration of 100 ppbv we mixed 0.06 L of the 10 ppmv N_2O (certified concentration: 9.95 ppmv + N_2 balance) @ 0.1 L/min. for 36 seconds, and 5.94 L N_2 (Research Grade, Nitrogen 6.0) @ 0.5 L/min. for 11 minutes 53 seconds. Similarly to make a 2% sample we used a 10% N_2O (certified concentration: 10.1% + N_2 balance) and N_2 .

For measurements of very low concentrations the polarization controller plates were adjusted carefully to obtain a stable laser line and pump current was adjusted to the threshold condition, so that the ASE close to the lasing wavelength became very sensitive to changes in loss from N₂O gas absorption lines in this region. Figure 6 shows the transmission spectra of reference gas N₂ and N₂O gas of concentration 100 ppbv. The gas mixture was prepared using the method described in the above paragraph. The measured concentration using Gas Chromatography was ~127 ppbv. Thus we conclude that the proposed system is capable of detecting N₂O gas at ppbv concentration levels. More experiments will be performed to find the lowest detectable limit using certified gas samples at lower concentrations [19].

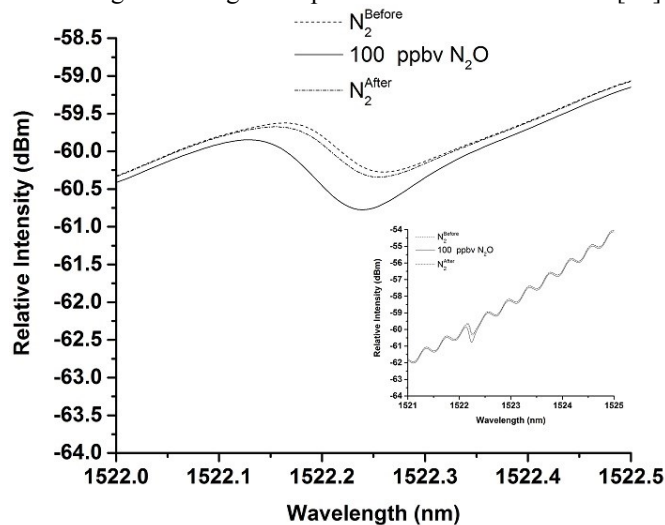


Fig. 6: Transmission spectra of the laser with reference gas N₂ and N₂O gas for $I_p = 130.0$ mA. The inset of the figure is the full spectrum.

In conclusion, we have demonstrated a fibre laser system that can detect N₂O concentrations ~ ppbv. The significant advancements are: (1) use of a FBG to allow operation in the shorter wavelength region of the ASE spectrum. (The FBG also reduces fluctuations in the ASE, and temperature stability may be achieved by maintaining the FBG at a fixed temperature or through an active stabilization scheme [20]). Further, one can select different absorption lines using a tunable grating; (2) stabilization against mode-hopping by use of a saturable absorber which also improves the accuracy of ASE measurements using the OSA; (3) use of an intra-cavity multi-pass gas cell to further enhance the sensitivity; (4) detection of N₂O at very low concentrations and (5) a targeted practical application in monitoring N₂O emissions from fertilizer in agriculture fields where the benefits of low power consumption and cost are important. It is expected that further work will reduce the minimum detectable concentration to even lower values.

References

[1] F. A. Phillips, R. Leuning, R. Baigenta, K. B. Kelly, and O. T. Denmead, "Nitrous oxide flux measurements from an intensively managed irrigated pasture using micrometeorological techniques,"

Agricultural and Forest Meteorology, vol. 143, no. 1-2, pp. 92-105, Mar.2007.

[2] A. J. Glenn, M. Tenuta, B. D. Amiro, S. E. Maas, and C. Wagner-Riddle, "Nitrous oxide emissions from an annual crop rotation on poorly drained soil on the Canadian Prairies," *Agricultural and Forest Meteorology*, vol. 166, pp. 41-49, Dec.2012.

[3] G. Whitenett, G. Stewart, H. B. Yu, and B. N. Culshaw, "Investigation of a tuneable mode-locked fiber laser for application to multipoint gas spectroscopy," *Journal of Lightwave Technology*, vol. 22, no. 3, pp. 813-819, Mar.2004.

[4] A. Campargue, D. Permogorov, M. Bach, M. A. Tamsamani, J. V. Auwera, M. Herman, and M. Fujii, "Overtone Spectroscopy in Nitrous-Oxide," *Journal of Chemical Physics*, vol. 103, no. 14, pp. 5931-5938, Oct.1995.

[5] L. Wang, V. I. Perevalov, S. A. Tashkun, B. Gao, L. Y. Hao, and S. M. Hu, "Fourier transform spectroscopy of N₂O weak overtone transitions in the 1-2 μ m region," *Journal of Molecular Spectroscopy*, vol. 237, no. 2, pp. 129-136, June2006.

[6] B. Gao, C. Y. Wang, Y. Lu, A. W. Liu, and S. M. Hu, "High-resolution infrared spectroscopy of N-15(2) O-16 in the 3500-9000 cm⁻¹ region," *Journal of Molecular Spectroscopy*, vol. 259, no. 1, pp. 20-25, Jan.2010.

[7] K. F. Song, A. W. Liu, H. Y. Ni, and S. M. Hu, "Fourier-transform spectroscopy of (NNO)-N-15-N-14-O-16 in the 3500-9000 cm⁻¹ region," *Journal of Molecular Spectroscopy*, vol. 255, no. 1, pp. 24-31, May2009.

[8] H. Y. Ni, K. F. Song, V. I. Perevalov, S. A. Tashkun, A. W. Liu, L. Wang, and S. M. Hu, "Fourier-transform spectroscopy of (NNO)-N-14-N-15-O-16 in the 3800-9000 cm⁻¹ region and global modeling of its absorption spectrum," *Journal of Molecular Spectroscopy*, vol. 248, no. 1, pp. 41-60, Mar.2008.

[9] R. A. Toth, "Line positions and strengths of N₂O between 3515 and 7800 cm⁻¹," *Journal of Molecular Spectroscopy*, vol. 197, no. 2, pp. 158-187, Oct.1999.

[10] A. W. Liu, S. Kassi, P. Malara, D. Romanini, V. I. Perevalov, S. A. Tashkun, S. M. Hu, and A. Campargue, "High sensitivity CW-cavity ring down spectroscopy of N₂O near 1.5 μ m (I)," *Journal of Molecular Spectroscopy*, vol. 244, no. 1, pp. 33-47, July2007.

[11] A. W. Liu, S. Kassi, V. I. Perevalov, S. A. Tashkun, and A. Campargue, "High sensitivity CW-cavity ring down spectroscopy of N₂O near 1.5 μ m (II)," *Journal of Molecular Spectroscopy*, vol. 244, no. 1, pp. 48-62, July2007.

[12] A. M. Parkes, A. R. Linsley, and A. J. Orr-Ewing, "Absorption cross-sections and pressure broadening of rotational lines in the 3 μ m band of N₂O determined by diode laser cavity ring-down spectroscopy," *Chemical Physics Letters*, vol. 377, no. 3-4, pp. 439-444, Aug.2003.

[13] E. Bertseva, A. Campargue, V. I. Perevalov, and S. A. Tashkun, "New observations of weak overtone transitions of N₂O by ICLAS-VeCSEL near 1.07 μ m," *Journal of Molecular Spectroscopy*, vol. 226, no. 2, pp. 196-200, Aug.2004.

[14] L. S. Rothman et al., "The HITRAN2012 molecular spectroscopic database," *Journal of Quantitative Spectroscopy & Radiative Transfer*, vol. 130, pp. 4-50, Nov.2013.

[15] V. M. Baev, Latz T., and Toschek P.E., "Laser Intracavity absorption spectroscopy," *Applied Physics B*, vol. 69, pp. 171-202, 1999.

[16] R. Bohm, A. Stephani, V. M. Baev, and P. E. Toschek, "Intracavity Absorption-Spectroscopy with A Nd³⁺-Doped Fiber Laser," *Optics Letters*, vol. 18, no. 22, pp. 1955-1957, Nov.1993.

[17] N. Arsal, M. Li, G. Stewart, and W. Johnstone, "Intra-Cavity Spectroscopy Using Amplified Spontaneous Emission in Fiber Lasers," *Journal of Lightwave Technology*, vol. 29, no. 5, pp. 782-788, Mar.2011.

[18] T. Hansch, A. L. Schawlow, and P. Toschek, "Ultrasensitive Response of a CW Dye Laser to Selective Extinction," *Quantum Electronics, IEEE Journal of*, vol. 8, no. 10, pp. 802-804, Oct.1972.

[19] H. P. Loock and P. D. Wentzell, "Detection limits of chemical sensors: Applications and misapplications," *Sensors and Actuators B-Chemical*, vol. 173, pp. 157-163, Oct.2012.

[20] Arsal N. and Stewart G., "Stable, tunable, and single-mode operation of an erbium-doped fibre laser system using a saturable absorber for gas spectroscopy applications," *SPIE 7195 ed 2009*, pp. 719525-1-719525-10.